8-20-2009

A new low-background Compton telescope using LaBr3 scintillator

Peter F. Bloser
University of New Hampshire, Peter.Bloser@unh.edu

James M. Ryan
University of New Hampshire, James.Ryan@unh.edu

Jason S. Legere
University of New Hampshire, jslegere@unh.edu

Manuel Julien
University of New Hampshire - Main Campus

Chris Bancroft
University of New Hampshire

See next page for additional authors

Recommended Citation

Peter F. Bloser ; James M. Ryan ; Jason S. Legere ; Manuel Julien ; Christopher M. Bancroft ; Mark L. McConnell ; Mark Wallace ; R. Marc Kippen and Shawn Tornga "A new low-background Compton telescope using LaBr3 scintillator", Proc. SPIE 7435, UV, X-Ray, and Gamma-Ray Space Instrumentation for Astronomy XVI, 74350H (August 20, 2009); doi:10.1117/12.826191; http://dx.doi.org/10.1117/12.826191

Authors
Peter F. Bloser, James M. Ryan, Jason S. Legere, Manuel Julien, Chris Bancroft, Mark L. McConnell, Mark Wallace, R M. Kippen, and Shawn Tornga

A new, low-background Compton telescope using $LaBr_3$ scintillator

Peter F. Bloser[a*], James M. Ryan[a], Jason S. Legere[a], Manuel Julien[a], Christopher M. Bancroft[a], Mark L. McConnell[a], Mark Wallace[b], R. Marc Kippen[b], Shawn Tornga[b]
[a]Space Science Center, University of New Hampshire, Durham, NH, USA 03824
[b]Los Alamos National Laboratory, Los Alamos, NM, USA 87545

ABSTRACT

Gamma-ray astronomy in the MeV range suffers from weak fluxes from sources and high background in the nuclear energy range. The background comes primarily from neutron-induced gamma rays, with the neutrons being produced by cosmic-ray interactions in the Earth's atmosphere, the spacecraft, and the instrument. Compton telescope designs often suppress this background by requiring coincidences in multiple detectors and a narrow time-of-flight (ToF) acceptance window. The COMPTEL experience on the Compton Gamma Ray Observatory shows that a 1.9-ns ToF resolution is insufficiently narrow to achieve the required low background count rate. Furthermore, neutron interactions in the detectors themselves generate an irreducible background. By employing $LaBr_3$ scintillators for the calorimeter, one can take advantage of the unique speed and resolving power of the material to improve the instrument sensitivity and simultaneously enhance its spectroscopic performance and thus its imaging performance. We present a concept for a balloon- or space-borne Compton telescope that employs deuterated liquid in the scattering detector and $LaBr_3$ as a calorimeter and estimate the improvement in sensitivity over past realizations of Compton telescopes. We show initial laboratory test results from a small prototype, including energy and timing resolution. Finally, we describe our plan to fly this prototype on a test balloon flight to directly validate our background predictions and guide the development of a full-scale instrument.

Keywords: gamma-ray astronomy, scintillators, $LaBr_3$, Compton telescopes, instrumentation

1. INTRODUCTION

Compton telescopes are the instruments of choice for spectroscopic imaging of the sky in the difficult energy range of 500 keV to 10 MeV[1]. This is so because the coincidence requirement greatly reduces the intrusion of single-photon and single-particle radioactive decays and scatters into the data. The intrinsic directionality of Compton telescopes further reduces background. The "classical" Compton telescope, COMPTEL[2], employed two detecting arrays separated by 1.6 m, with a good event having near simultaneous interactions in the two detectors. Compton scatters in the forward detector D1 were measured for location, energy deposit and pulse shape. D1 was composed of liquid organic scintillator. Location and energy deposit were measured for scatters into the rearward detector D2 and the time-of-flight (ToF) was measured between the detector triggers. D2 was composed of NaI(Tl). From the positions and energy deposits in the two detectors, the source of the incident gamma-ray photon could be constrained to lie on an "event circle" on the sky using the Compton scattering formula. The coincidence requirement greatly reduced the effective area of the instrument, but reduced the background even further, yielding a net improvement in sensitivity over single detector systems. COMPTEL produced the first map of ^{26}Al in the galaxy, discovered AGN emission in the MeV range, measured prolonged gamma-ray emission from solar flares, and much more, including a measure of the cosmic diffuse flux in the 1-30 MeV range.

The achievements of COMPTEL, although impressive, were not as good as what was expected before launch. This shortcoming can be entirely attributed to an elevated level of background, relative to what was expected. Roughly speaking, the unexpected background increase was of order four. The reasons for this will be described below; however, one can significantly advance the sensitivity of these instruments by directly attacking all the major sources of background experienced by COMPTEL. Many of these improvements can be demonstrated in a balloon flight. New technology, combined with the experience from the COMPTEL experiment, will allow us to retain a simple scintillator configuration while simultaneously greatly reducing the effects of background sources, which ultimately limited the achievements of COMPTEL, while reducing the cost[3]. Furthermore, these new technologies provide for energy and angular resolutions that are two to three times better than COMPTEL.

* Peter.Bloser@unh.edu; phone +1-603-862-0289; fax +1-603-862-3584

UV, X-Ray, and Gamma-Ray Space Instrumentation for Astronomy XVI,
edited by Oswald H. Siegmund, Proc. of SPIE Vol. 7435, 74350H · © 2009 SPIE
CCC code: 0277-786X/09/$18 · doi: 10.1117/12.826191

Much work has been devoted to the study of a concept known as the Advanced Compton Telescope (ACT), a visionary mission that could take place sometime after 2015. Many new designs for Compton telescopes were put forward in a recent Concept Study for ACT[4,5]. The science goal of ACT, out of necessity, was narrowly and ambitiously defined to measure the intensity and shape of gamma-ray lines (specifically the 847 keV line from ^{56}Co) from distant Type Ia supernovae. This narrow requirement led to a baseline ACT design employing great numbers of Si and Ge semiconductor detectors, cooled to cryogenic temperatures, with a cost of at least $800 million. However, we feel that, before initiating such a large, narrowly focused mission, it is necessary to expand and deepen the medium-energy gamma-ray scientific database with a sensitive survey mission. Major improvements in all of MeV astrophysics will be possible with a "general purpose" scintillator-based instrument at a manageable cost. To accomplish this, we must understand at an elementary level the technology necessary to mitigate the major background sources experienced by COMPTEL. Here we describe our program to develop such technology, based on new fast scintillators, and to incorporate it into a sensitive instrument suitable for an ultra-long duration balloon payload or Explorer mission.

2. SCIENTIFIC MOTIVATION

We strongly believe that the top near-term scientific priority for MeV astronomy is a comprehensive all-sky survey with an order of magnitude improvement in sensitivity over COMPTEL for both line and continuum sources. A broad range of astrophysical science is best studied via observations in the so-called medium-energy gamma-ray band, from roughly 0.4–10 MeV. Medium-energy gamma rays probe extreme physical conditions in the Universe that give rise to nuclear interactions and relativistic particles. COMPTEL was able to detect a few examples of various types of astrophysical sources in this energy band, but not enough to study a representative sample of any source class. A true astronomical survey of the MeV sky is therefore desperately needed. COMPTEL provided only a dim, blurry view of the MeV Universe, but it was sufficient to demonstrate that the science return of a more sensitive survey instrument will be rich. Science to be studied with a sensitive Compton telescope includes:

2.1 Relativistic Particle Accelerators:

Black-hole candidates and *active galactic nuclei* (AGNs) exhibit emission in the MeV range, probably from the re-energization of X rays by scattering off high-energy electrons. The MeV tail on the spectrum of Cyg X-1[6] represents the exciting physics that can emerge when studying such objects. AGNs have been associated more with emission above 100 MeV, but this is likely due to the limited sensitivity in the MeV band. A broader picture of AGNs will probably emerge when more are measured in the MeV band with more so-called MeV blazars being identified. The object 3C273 is such an example of an AGN that is luminous in MeV gamma rays.

Pulsars should be common in the Galaxy if one has the sensitivity to detect them. COMPTEL detected a handful of them, all displaying different behaviors in spectrum, light curve and frequency. This diversity makes categorizing them difficult. A larger set of gamma-ray pulsars might exhibit trends that could be used to understand them.

Gamma-ray bursts exhibit some of their most interesting features at energies higher than the classical 100-200 keV band. Long bursts on the time scales of an hour at GeV energies[7] have been recorded, but studies of their long-term behavior at MeV energies have been limited by sensitivity.

Solar Flares exhibit the most complex spectra in the sky. The richness of nuclear lines, bremsstrahlung emission, positron annihilation, and neutron capture contains much information about the processes of ion acceleration that produces these lines. Because of the complexity of the spectrum, the diagonal instrument response of a Compton telescope will greatly aid in the interpretation of the data.

Many of the phenomena described above probably produce gamma radiation that is at least partially *polarized*. A gamma-ray telescope based on Compton scattering is in principle sensitive to polarization and thus offers a new diagnostic tool for the study of high-energy astrophysical processes[8].

2.2 Nuclear Astrophysics

The *radioactive isotope* ^{26}Al populates the plane of the Galaxy, producing a diffuse Galactic emission. ^{26}Al was mapped using COMPTEL data[9], but higher definition versions of these maps are necessary to properly associate the emission with distinct galactic structures and their progenitor stars. A similar map of the fainter ^{60}Fe emission is needed for comparison and correlation studies.

Measurements of radioactive decay line emission from *supernova remnants* (SNR) are scientifically valuable. Improving upon the COMPTEL ^{44}Ti luminosity measurements of Cas-A[10] would be accompanied by luminosity measurements of ^{26}Al and ^{60}Fe. These isotopes drive the last phases of the supernova expansion and populate the Galaxy with radioactive ash. *Classical novae* produce isotopes that radiate in the MeV range that can constrain the dynamics of the origin of lighter elements.

Search for and measurement of *supernova* (SN) emissions to better understand the dynamics of the explosion process and the creation of the elements is a top priority. The anomalous redshift velocities of distant Type Ia SNe have led to a critical review of the cosmological constant. It is important to fully understand the Type Ia process since it is used here as a standard candle to evaluate the Hubble constant. COMPTEL was able to place upper limits on ^{56}Co gamma-ray line emission from one SN and marginally measure another[11]. With a 10× improvement in sensitivity, it is likely that a Type Ia SN will occur in a five-year period within a radius where good measurements can be conducted so as to test our models of the phenomenon.

2.3 Diffuse Continuum Emission

The origin of the *diffuse Galactic continuum* emission at MeV energies is still mysterious: current models of galactic gamma-ray production in cosmic-ray/gas interactions fail to provide a satisfactory explanation for this galactic glow[12].

The spectrum of the *cosmic diffuse gamma* (CDG) emission derived from COMPTEL, EGRET and SMM data appears to be composed of several components. These components include active galaxies and supernovae. The supernova component is the least resolved and understood. A new mission would greatly improve on the COMPTEL measurements of this spectrum from below 1 MeV to 10 MeV and help establish the magnitudes of the different contributions.

These science goals require both line and continuum sensitivity, as well as sensitivity to both point and extended sources. To accomplish these diverse scientific goals a new, "general purpose" telescope design superior to that of COMPTEL is necessary, and to do that the background rate must be reduced.

3. TECHNICAL ISSUES: COMPTON TELESCOPE BACKGROUND AND ITS SUPPRESSION

Scintillator-based Compton telescopes have flown on balloons as far back as the late 1960s[13,14,15]. All achieved success, to different degrees, in conducting astrophysical studies. These endeavors ranged from MeV measurements of secondary neutral cosmic radiation to measurements of the Crab and Vela pulsars and the Crab nebula, to mapping, albeit crudely, of the ^{26}Al galactic radiation, to the cosmic-diffuse flux. However, with the COMPTEL experiment, this basic design ran up against the limits of background that one experiences on a space platform. In the end, it was the inability to deal with the COMPTEL background rate, that was of order 4× above early estimates, that limited the scientific return from the mission, because many sources were no longer statistics limited. In fact, in the most problematic energy ranges, it was the unavoidable and uncontrolled background fluctuations that limited the instrument sensitivity, rather than photon statistics[16]. However, on the bright side, the instrumental background was exhaustively studied and cataloged as part of the measurement of the MeV cosmic-diffuse background. Without introducing new channels of background, steps can now be taken to mitigate all major components of the instrumental background that plagued COMPTEL, enabling a modern re-design that can achieve far greater sensitivity and improved angular and energy resolution performance. First we describe the historical methods, both in hardware and analysis, for excluding background in the COMPTEL experiment. We then describe, in some detail, (1) the physical nature of the COMPTEL background, and (2) new methods in hardware that can mitigate the effect of these sources of instrumental background.

A cutaway schematic of COMPTEL is shown in Fig. 1, showing the upper liquid organic scintillator array D1 and the lower NaI crystalline detector array D2, 1.6 m (light travel time 5 ns) from D1. Also shown is a typical Compton scatter kinematic diagram showing that without measuring the momentum vector of the recoil electron in D1, the incident direction of the photon is constrained to lie on the mantle of the cone with its axis being the unit displacement vector from D2 to D1 with a half angle ϕ—the scatter angle.

The hardware methods used for reducing background in COMPTEL were (1) charged particle shields to exclude effects of proton and electron induced prompt gamma rays, (2) time-of-flight with a final (after processing) 4-ns coincidence window that restricted events to forward directions and eliminated single triggers for photons and radioactive decays, and (3) pulse-shape-discrimination in D1 that reduced the effect of inelastic neutron scatters off carbon in the organic scintillators.

In the data analysis and processing, we selected events in the forward ToF interval, the electron-pulse-shape interval, and events that had relative energy deposits in D1 and D2 that correspond to Compton scatters less than (typically) 36˚. Finally, the resulting event circle for each event was not allowed to come closer than 10˚ to the horizon. These losses of

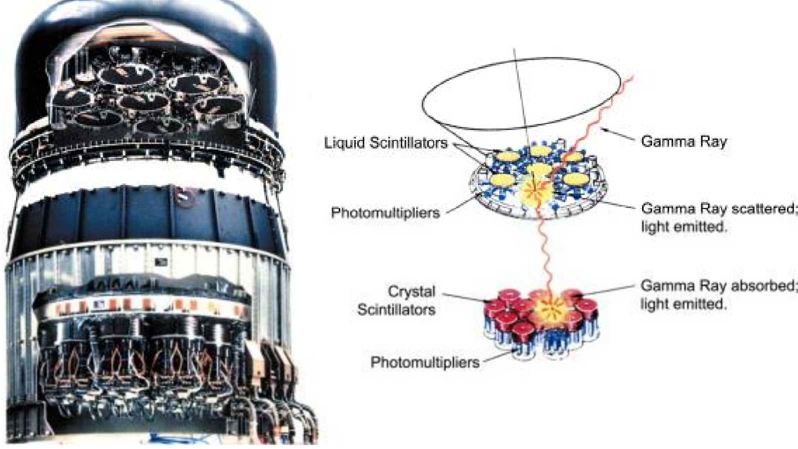

Fig. 1. COMPTEL cutaway view with Compton scatter kinematics.

solid angle significantly reduced the effective area of the instrument. The remaining events constituted the highest quality events that were then fed into imaging and spectroscopic studies.

The hardware and on-board software restrictions reduced the on-board count rate (in deep space observations) to ~10 Hz from 0.75 to 30 MeV. Ground software data cuts further reduced the count rate to ~5 Hz. This should be compared to the expected cosmic diffuse true event rate of ~1 Hz. If one can reduce the background rate to the same order as that of the cosmic-diffuse flux or lower, uncontrolled background fluctuations will give way to photon statistics as the driving factor in sensitive observations.

3.1 The Physical Nature of the COMPTEL Background

One of the goals of instruments in this energy range has always been to accurately measure the so-called MeV cosmic-diffuse background flux, an unresolved, but intense, cosmic radiation field of uncertain origin. Because no structure has been observed and little expected in this energy range, imaging is of little value. Rather, to measure the spectrum, all steps must be taken to minimize the background, thereby maximizing the signal-to-noise ratio. A major loss of effective area could always be made up with long exposures. Measuring the cosmic-diffuse gamma-ray spectrum is the test case for any MeV instrument.

In the course of these investigations with COMPTEL[17,18,19] much was learned about the nature of the Compton telescope background, i.e., the limiting factor in these measurements. We learned that although the sensitivity to single photon backgrounds, such as that from radioactive ^{40}K contamination in photomultiplier tube glass, was virtually eliminated by the double Compton technique, prompt double-photon background produced in the instrument and single photon background production in the detector elements themselves proved to be the limiting factors for the instrument sensitivity.

For example, ^{22}Na emission from activation in the D2 detector (NaI based) was never detected in the main data stream even though its production is well documented in the GRS of SMM[20] and in OSSE on the Compton Observatory. The gamma rays from ^{22}Na decays could easily be rejected because they had a unique ToF signature, i.e., they traveled in the wrong direction. However, photons from ^{24}Na and ^{22}Na produced in the activated aluminum of the D1 detector housing were a persistent, time variable and elusive background affecting all measurements below 4 MeV[16]. ^{24}Na was a problem because the isotope emits two simultaneous photons of 1.37 and 2.75 MeV with one triggering D1 and the other triggering D2. The ToF signature was almost exactly what one expects from a cosmic gamma ray. However, upon close inspection, slight distortions were seen in the ToF spectrum of otherwise good photons. The distortions were in the direction of slightly smaller ToF values than normal, indicating that the second photon of the ^{24}Na cascade was part way to D2 when the first photon triggered D1.

The other major problem was that the organic scintillators used in D1 and the charged particle shield thermalized and captured free neutrons produced by cosmic-ray interactions in the instrument, spacecraft or Earth's atmosphere. The result was a strong neutron-capture 2.223-MeV emission line in the aperture of the instrument. These photons properly scattered and could not be distinguished from otherwise good cosmic photons. This adversely affected all measurements at and below 2.2 MeV.

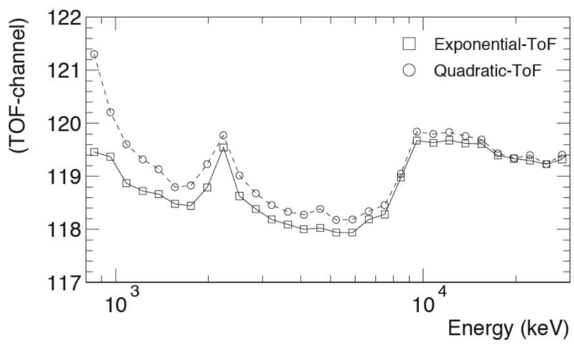

Fig. 2: Centroid of the COMPTEL ToF peak as a function of energy.

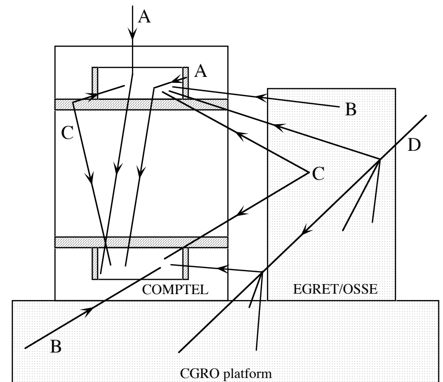

Fig. 3: The major types of background events in COMPTEL (see text).

These two effects can be seen in the COMPTEL mean-ToF plot as a function of measured gamma-ray energy in Fig. 2. Plotted in Fig. 2 is the centroid of the ToF peak for the highest quality events in the COMPTEL data stream. The ToF channel of a good cosmic gamma ray for COMPTEL was, by design, 120. As evident in Fig. 2, this was satisfied for energies of 2.2 MeV and above 9 MeV. At all other energies the centroid was always below 120, indicating that double-photon cascade background was contaminating the data. The ToF centroid was correct at 2.2 MeV because those photons were intense and true double scatters, while above 9 MeV there are few nuclear states to provide a double-photon cascade. For other energies, the offset of the centroid is more than 500 ps from the proper mean-ToF value. This can be understood because a single D1 detector cell had a radius of 14 cm or ~500 light-ps. Cascades initiating in the housing or platform of a D1 cell would typically travel for 500 ps before scattering in a D1 cell. In this time the other photon of the cascade was 14 cm on its way toward D2, thereby registering as a coincidence ~500 ps off the proper ToF. More detailed analyses of the ToF spectrum[17,18] resolved this double-photon cascade component, placing it almost a full 1 ns away from the proper cosmic-photon value. COMPTEL with its 1.5-ns ToF resolution had a difficult time dealing with this background component since the two ToF distributions merged into a single Gaussian-looking feature. However, one can imagine a Compton telescope with a ToF resolution of ~400 ps or better neatly resolving the cascade background from the cosmic flux—meaning that only cascades initiating a few cm or less from a D1 cell would contaminate the data.

Cosmic-ray interactions in the instrument, spacecraft, or the nearby Earth's atmosphere produce an intense neutron radiation field. The neutrons would often thermalize in and around the D1 detector. Once inside a D1 cell they would combine with hydrogen to form deuterium, releasing the deuteron binding energy in a single photon with energy of 2.223 MeV that could, in turn, double scatter and enter the data stream. Organic scintillators with similar properties to those used in COMPTEL are available with hydrogen replaced by deuterium. A Compton telescope using deuterated organic scintillators (in D1 and in the surrounding charged particle shields) would be immune from this form of background.

The major background events types in COMPTEL are illustrated in Fig. 3[17]. Sub-ns ToF resolution measurements can eliminate all the event types shown except Type A and a small fraction of Types B & C. Type A events include (1) neutron captures on hydrogen in the organic scintillator of D1, (2) neutron capture on hydrogen in the organic scintillator of the forward charged particle shield, (3) single photon penetration of a D1 cell (cosmic gamma rays) and (4) photons from inelastic neutron-carbon scatters with the carbon decaying to the ground level. Lastly, activation of the carbon in the organic scintillator of D1 can produce events. In particular ^{11}C emits a β^+ particle in D1 with a subsequent 511 keV photon triggering D2. Type B events inside the ToF window and Type C events occurring close to D1 are also not eliminated entirely. Many of these events can, however, be eliminated by restricting the computed scatter angle. For example, virtually all of the ^{11}C events in COMPTEL were eliminated because of the large positron energy deposits in D1 relative to the energy deposited in D2, implying a large Compton scatter if it were a cosmic gamma ray. Similarly, ^{40}K photons from the glass of the photomultiplier tubes (PMTs) must undergo a large scatter in D1 to make it to D2. These cuts were effective—no signal from ^{12}C, ^{11}C, or ^{40}K was detected in the COMPTEL data stream.

3.2 New Methods in Hardware

Several lessons can be learned from the COMPTEL experience. These include (1) the ToF resolution must be as small as possible. This reduces the frequency of Type B events and reduces the susceptible volume of Type C events to that very close to D1. For example, shown in Fig. 4[17] is the highly selected ToF spectrum from 4.2 to 6 MeV used in the CDG analysis. The energy band was chosen as a worst case, because it is free of weak-decay radioactive contamination (Type C events). Shown are the fitted Gaussian curves for good Type A events and Type C events, i.e., *prompt* cascade events with systematically small ToF values. The Gaussian rides on top of the Type C continuum and the continuum from accidental coincidences, all of which are accepted in the ToF window. Fig. 5 shows the expected ToF curves from an instrument with a 400 ps ToF resolution. The components are now resolvable. New instrument geometries can be envisioned and evaluated to ensure that these components remain resolvable, while optimizing other instrument parameters, such as efficiency. A side benefit of a small ToF resolution is that that the individual D1 and D2 cell volumes must be small, thereby increasing the light collection efficiency, improving energy resolution, and improving the spatial resolution.

Lesson (2) is that the passive mass surrounding D1 (and only D1) be small and of a composition that resists activation and has few multi-photon cascade channels. For example, a space flight mission might use Be instead of Al. A lower-cost option would be to use Mg to reduce the mass near D1, although activation, even in the reduced mass, would still be an issue.

Lesson (3) is that the overlying material in the aperture is a limiting factor for sensitivity. Locally produced neutrons will make this material glow in MeV gamma rays, and those photons will properly scatter in the instrument and cannot be removed by any means, "fogging the film" of the observation. A corollary to this is that regardless of the technique used, either in hardware or software, the gamma sensitivity, either broad-band, line or point or extended source is ultimately limited by the gamma ray luminosity of the overlying passive material in the aperture of the instrument. This material takes the form of micrometeorite shielding, thermal blankets and light-tight covers, all required in space missions. Charged particle detectors are not part of the problem, because they register most of the neutron and/or proton interactions that could produce secondary gamma rays. In particular, neutron sources must be far away from this material. These sources include the Earth's atmosphere and the spacecraft itself. Positioning the spacecraft well away from the Earth and deploying the telescope from the supporting spacecraft by an umbilical minimizes the neutron intensity on the sensitive material in the forward scatterer assembly and the overlying passive material.

Finally, (4) eliminate hydrogen in D1 and the forward charged particle shield. This involves using deuterated organic scintillators. The hydrogen in the organic scintillators radiates 2.223-MeV gamma rays. If all the hydrogen is in the form of deuterium, the 2.223-MeV radiation is eliminated.

The effect of carbon in D1 is not easily reduced, but indications are that this is not a major effect in any case. For example, no 4.43 MeV line has ever been detected in the COMPTEL background, placing an upper limit on the intensity of this component.

To summarize: the actions that can greatly affect the background count rate without affecting efficiency are (1) reduce the ToF resolution with a goal of 400 ps or better, (2) employ deuterated pulse-shape sensitive organic scintillators in

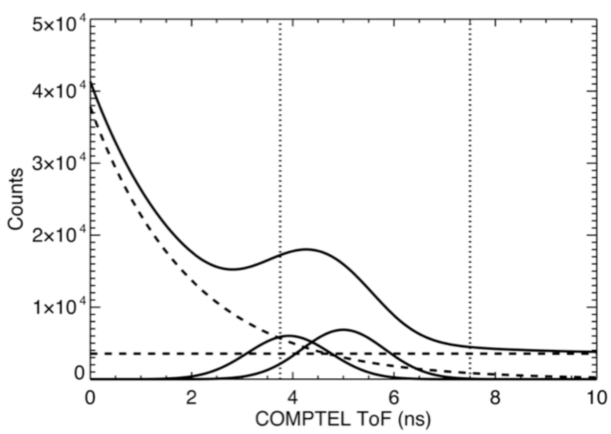

Fig. 4. COMPTEL ToF spectrum from 4.2-6 MeV. Components are described in the text. Dotted vertical lines indicate ToF window for good events.

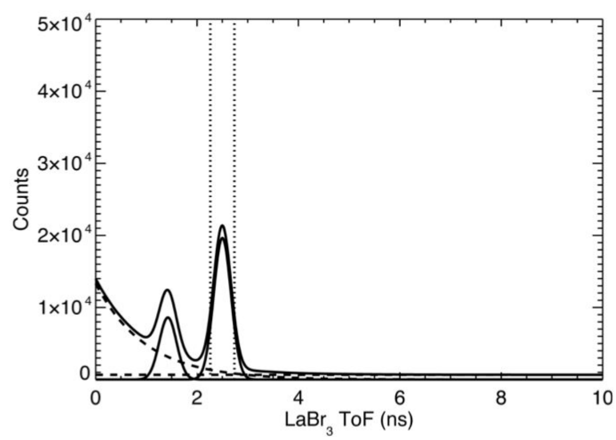

Fig. 5. Estimated ToF spectrum of a Compton telescope using $LaBr_3$ for D2. Components are scaled from Fig. 4 as described in the text (see Sec. 4).

strategic locations and (3) reduce the mass immediately above and surrounding D1, ideally with a composition resistant to activation. Below we describe the expected reduction in background rates for the various event types in one possible configuration.

4. A NEW DESIGN USING ADVANCED SCINTILLATORS

The requisite improvement in detector performance (fast timing, good energy resolution, good stopping power) can now be realized with modern fast scintillator materials. One promising material that has been the subject of intense study in recent years is cerium-doped lanthanum bromide ($LaBr_3$:Ce)[21]. Compared to "traditional" scintillators such as NaI(Tl) (used in COMPTEL D2), $LaBr_3$ offers greater light output (60,000 vs. 49,000 photons MeV^{-1}), higher density and stopping power (5.1 vs. 3.7 g-cm^{-3}), faster response (1/e decay time of 16 ns vs. 250 ns), and superior energy resolution (2.8% vs. 7% FWHM at 662 keV)[21]. In addition, ToF resolution less than 250 ps (FWHM) has been measured between $LaBr_3$ detectors and other fast scintillators[22,23]. $LaBr_3$ is under study by many groups for space applications, including deep space missions[24]. Deuterated liquid scintillator is also commercially available.

We have developed a baseline conceptual model of a modern Compton telescope utilizing modern scintillators for improved efficiency, timing, energy resolution, and background rejection. A subsection of the model is shown in Fig. 6. The model comprises 2 layers of deuterated liquid scintillator for D1 and 2 layers of $LaBr_3$ detectors for D2. Each layer is 100 cm × 100 cm, and the separation between D1 and D2 is 75 cm. Each individual D1 or D2 detector element is a 2-cm cube. No finer spatial resolution is assumed, because we wish to study the performance achievable with excellent time resolution and good energy resolution while keeping the channel count modest. The mass equivalent of a compact PMT (glass, Be, and Cu) is placed adjacent to each detector element (above the top layer and below the bottom layer). A thin plastic scintillator shield surrounds the D1 and D2 detector planes. We assume the measured values for detector energy resolution (@ 662 keV in each detector) given above, and a trigger threshold of 20 keV in both D1 and D2. We assume a ToF resolution of 400 ps for the $LaBr_3$ D2.

To estimate the sensitivity of an instrument based on the modern scintillator technology described above, we have performed initial simulations of the response of a Compton telescope using the MGGPOD Monte Carlo package[25]. We first simulated mono-energetic photons at five different energies (511 keV, 847 keV, 1.809 MeV, 4.438 MeV, and 6.130 MeV) with normal incidence to predict the telescope response (energy resolution, angular resolution, and effective area A_{eff}). Simple data cuts were used: events were allowed if there was exactly one trigger in D1 and either one or two triggers in D2. In the case of two D2 triggers, the hit in the top D2 layer was assumed to be the first. The computed Compton scatter angle was required to be in the range 0-53°. The results are plotted in Figs. 7–9. The dotted line indicates the values from COMPTEL calibration measurements[2]. The angular resolution is given in terms of the angular resolution measure (ARM), the difference between the computed and true scatter angles. The effective area is given for events falling within 3σ-wide windows around the incident energy, a ToF value of 2.5 ns, and an ARM of 0°. A Compton telescope of this size based on $LaBr_3$ will significantly outperform COMPTEL in energy and angular resolution. Below ~2 MeV an equal or significantly larger effective area can be achieved. This is impressive performance for an instrument less than 25% the volume and mass of COMPTEL. At higher energies the effective area of this telescope suffers due to the thin D2.

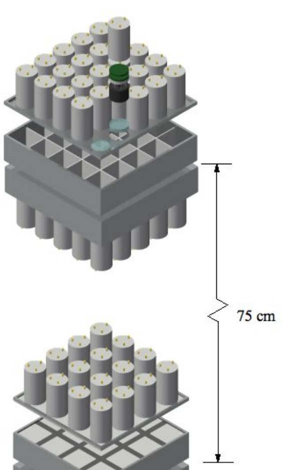

Fig. 6. A 10 cm × 10 cm subsection of the model Compton telescope using deuterated liquid scintillator for D1 and $LaBr_3$ for D2.

To estimate the magnitude of the background reduction we might expect, we examined a sample ToF spectrum from COMPTEL. We focused on the most difficult background range to improve, that of 4.2–6 MeV. Although the absolute background rate is low compared to other bands, this range suffers from a continuum background with no spectral features to aid in its removal. Fig. 4 shows the COMPTEL ToF spectrum from 4.2–6 MeV used in the CDG analysis[17]. Because our proposed methods will have the greatest effect on activation background, we chose this energy interval because it sits above all the activation lines, thereby making it the most challenging energy range for improvement. However, it is

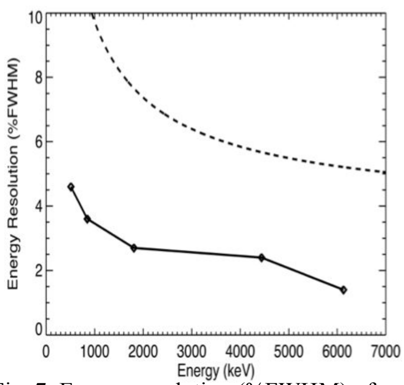

Fig. 7: Energy resolution (%FWHM) of the $LaBr_3$ scintilator Compton telescope vs. energy. Dotted line indicates values for COMPTEL.

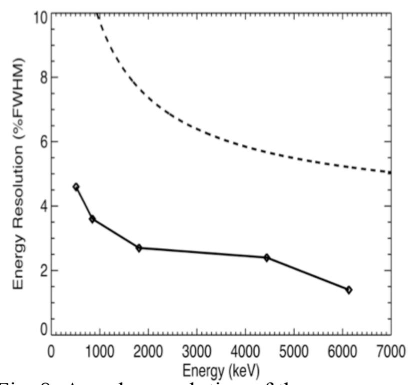

Fig. 8: Angular resolution of the scintillator Compton telescope as measured by the ARM. Dotted line indicates values for COMPTEL.

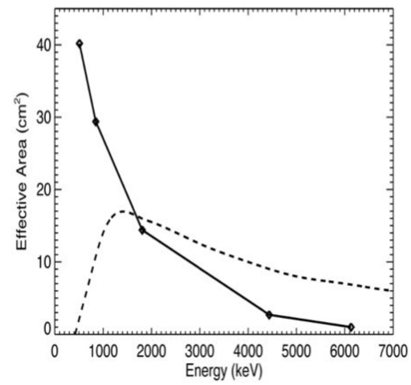

Fig. 9. Effective area of the example scintillator Compton telescope for the data cuts given in the text. Dotted line indicates values for COMPTEL.

important to note that more fertile ground for background rejection lies below this range. Below 4.2 MeV, the background rejection techniques we discuss can be employed to make very large improvements. Because of the absence of radioactive contamination, the energy range from 4.2–6 MeV represented COMPTEL's best performing range. It falls above the intense contamination from ^{24}Na, ^{22}Na, ^{28}Al, and neutron capture (2.2 MeV). The primary background here comes from prompt neutron cascades in material in the aperture of the instrument (along with accidental coincidences and cascades from elsewhere in the instrument and spacecraft, which we will eliminate via ToF discrimination). The different background components are shown as fitted: Type A events (right Gaussian), Type C events near D1 (left Gaussian), Type B events (constant), and Type C & D events from the rest of the instrument (exponential continuum). The Type A events with the proper ToF are gamma rays coming down the boresight of the instrument produced in the field of view by undetected neutrons. They constitute the most elusive form of background. We have conservatively estimated how these background components might rescale in a telescope with $LaBr_3$ (Fig. 5) for D2 on the assumption that count rates scale with detector mass. We reduced the Gaussian widths to match the assumed ToF resolutions and those peaks were rescaled by the ratio of the total D1 mass to the COMPTEL D1 mass. The Type C events were further reduced by a factor of two to allow for the use of a material, such as Be, less subject to activation. The Type D continuum was scaled by the ratio of the overall telescope mass, which we conservatively assumed would scale as the ratio of the detector masses. The Type B events were scaled by the product of the D1 and D2 mass ratios. The number of counts within the valid ToF window (vertical dotted lines) was then compared to that of COMPTEL. The only significant remaining background is from Type A events. This simple estimate yielded roughly a factor of 2.5 reduction in background assuming that the amount of passive material in front of D1 remains unchanged in quantity and composition. This is the reduction expected for observations of isotropic, continuum sources such as the CDG in the energy range 4.2–6 MeV. To see how this would affect the sensitivity for point-line sources, we scaled this background by the ratio of the permitted energy (Fig. 7) and ARM (Fig. 8) windows, as appropriate for observations of point-like, line sources (e.g., SNe, SNR, knots of ^{26}Al or ^{60}Fe emission, etc.). This gives a rough estimate of the background reduction possible with the baseline Compton telescope model: a factor of ~20 for a $LaBr_3$ D2. Using the simulated effective areas we may also estimate the relative line sensitivity to a point source located on-axis. At 1.809 MeV, assuming the background scales as it does from 4.2–6 MeV (a conservative overestimate), we expect to improve on the COMPTEL sensitivity (in units of σ) by a factor of ~4 ($LaBr_3$). In effect, we use the good ToF resolution of this instrument to reduce background in the same manner that Ge detectors use its good energy resolution to reduce background.

This sensitivity estimate represents a "worst case" comparison and we expect to do much better in practice, especially in the ranges of radioactive isotopes that have spectral signatures to aid in removal. The background reduction was estimated from COMPTEL's best performance energy band, whereas below 4.2 MeV the reduction would be significantly greater due to the activation background that plagued COMPTEL. The largest background component remaining, the Type A events, arises from neutron interactions in passive material in the telescope aperture. This can be reduced by aggressively limiting this passive material. Additional reduction factors of a few can be expected because of the absence of the EGRET and OSSE telescopes and the selection of a low-inclination or deep space orbit (the CGRO orbit was at ~28°) that prevents SAA activation. Finally, we note that Type A events will be a significant, inescapable source of background in any Compton telescope design, and that liquid organic scintillator offers far fewer decay chains than higher-Z detector materials. Given these considerations, we find the factor of ~4 improvement in sensitivity derived using the relatively clean range of 4–6 MeV encouraging. We estimate that the background problem is four times worse in the range of 2.7–4.2 MeV and about twice as bad from 1.5–2.7 MeV judging from the COMPTEL S/N ratio of background count rate to cosmic diffuse count rate. Thus, for objects that radiate in these ranges large improvements are possible using the techniques described above, especially if their spectrum is harder than the cosmic diffuse spectrum (e.g., lines). At the higher energies the segmentation of the detectors will improve the imaging properties of the detector, because both the mean free path of a Compton scattered photon and sometimes the range of the scattered electron will be comparable to or greater than the segmentation size. Knowing where the reactions were initiated to 2 cm will reduce the geometrical uncertainties in the imaging exercise. We have not estimated the magnitude of this advantage over the COMPTEL instrument at this point, but it will improve with energy.

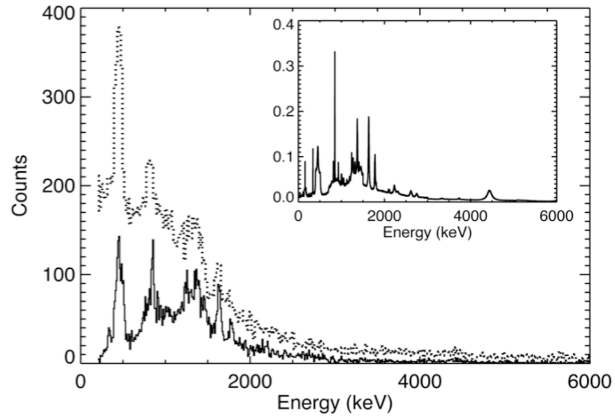

Fig. 10. Simulated solar flare spectrum (inset) as measured by the $LaBr_3$ Compton telescope (solid) and monolithic NaI detector (dotted).

The improved energy resolution, with respect to COMPTEL, is achieved with small detector volumes with large PMT coverage and the use of high-resolution scintillators such as $LaBr_3$. The energy resolution is slightly degraded from pure $LaBr_3$ because small amounts of energy are deposited in the liquid scintillator. Despite this, we have simulated the complex count-rate spectrum from a solar flare and compared it to that recorded using a bare monolithic 3″ × 3″ cylindrical NaI detector, the material used by both GRS on SMM and OSSE instruments (Fig. 10). Not only are the individual lines much narrower, but after selecting events based on imaging information, the suppression of the Compton tails is quite significant (compare to the input spectrum, shown in the inset). This enables one to much more easily and unambiguously de-convolve the complex solar spectrum of narrow lines, broad lines and continuum. This power could be applied to any Type Ia spectrum measured, thereby ruling out many conflicting models. Much SN progress can be made with ~3% energy resolution at 847 keV, because the ^{56}Ni lines are separated by more than this (~4%) and they vary significantly in intensity depending on the model and the age of the SN. The lines themselves are Doppler broadened at the 3% level.

5. LABORATORY DEVELOPMENT AND BALLOON FLIGHT TEST

We are currently preparing a laboratory prototype of a Compton telescope using deuterated liquid scintillator for D1 and $LaBr_3$ for D2. We will directly measure the ToF resolution, energy resolution, and test the background rejection using strong radioactive gamma and neutron sources. We will then fly this prototype on a balloon test flight to directly test the background rejection capabilities. This balloon flight will make use of hardware previously flown as part of a test flight of the GRAPE gamma-ray polarimeter project[26]. We expect this test flight to take place in the fall of 2010.

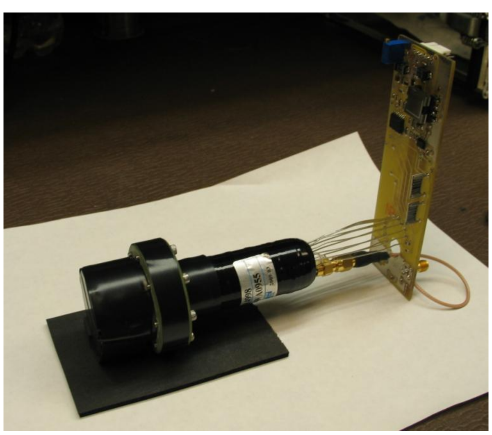

Fig. 11. Laboratory prototype D1 cell, showing Teflon™ housing for deuterated liquid, R4998 PMT, and custom HV/preamp board.

5.1 Laboratory Prototype and Initial Results

The prototype will consist of 2 – 3 detector cells in both D1 and D2. The cells will each be 1″ × 1″ cylinders, consisting of deuterated liquid scinillator (EJ-315 from Eljen Technology) in D1 and $LaBr_3$:Ce (BrilLanCe™ 380 from Saint-Gobain Crystals) in D2. At the present time we have constructed and tested one D1 cell, using Teflon™ and OP.DI.MA.™ reflector material from Gigahertz-Optik GmbH for the housing in order to avoid high-Z materials. We have also tested one D2 detector using a 0.5″ $LaBr_3$ crystal available from another project; two 1″ crystals are on order from Saint-Gobain. Both the D1 and D2 scintillators are read out using fast, 1″ R4998 PMTs from Hamamatsu Corp. Custom high-voltage (HV) supplies and preamplifiers were designed and fabricated for each detector. Fig. 11 shows the D1 cell, PMT, and HV/preamp board. Standard laboratory electronics, including a constant-fraction discriminator, amplifiers, time-to-amplitude converter, coincidence unit, and analog-to-digital converters were used for data acquisition, controlled by a LabView™ interface.

We initially measured the ToF resolution using two 0.5″ $LaBr_3$ detectors coupled to two R4988s in order to determine the "best case" performance achievable using these PMTs and to characterize how the resolution depended on the HV. The detectors were placed approximately 15 cm apart with a ^{22}Na source between them, and only events corresponding to coincident 511 keV photopeak events in both detectors were included. The HV on one PMT was kept at 2000 V, and the other HV was varied. The results are shown in Fig. 12. With both PMTs at 2000 V a ToF resolution of 264 ± 3 ps (FWHM) was achieved, consistent with results reported elsewhere[22,23]. At this HV, however, the linear dynamic range for the $LaBr_3$ was severely limited due to its high light output and fast response. Achieving a linear range extending to ~20 MeV required that the HV be reduced to 1500 V; this implies a maximum ToF resolution of ~350 ps (Fig. 12).

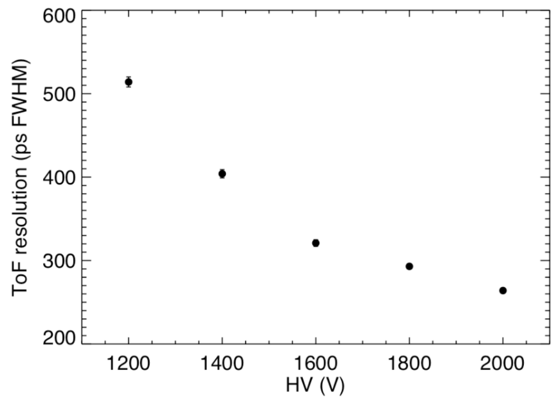

Fig. 12. Time-of-flight resolution for 511 keV events measured between two $LaBr_3$ detectors coupled to R4998 PMTs. One PMT was kept at 2000 V and the other varied.

We next measured the ToF resolution between the D1 cell, with the HV turned up to 2300 V to maximize the gain due to the lower light output of the liquid, and a $LaBr_3$ D2 cell with the HV reduced to 1500 V. We selected on 511 keV photopeak events in D2 and the Compton edge, corresponding roughly to 340 keV, in D1. This yielded a ToF resolution of 695 ps (FWHM). We expect to improve on this value by optimizing the light output from the D1 cell and by obtaining the D2 signal from a dynode rather than the anode. This will allow us to reduce the gain without lowering the HV in the PMT. We note, however, that a ToF resolution of ~700 ps is already a factor of ~3 better than that of COMPTEL.

We next recorded Compton-scatter data between D1 and D2 using a ^{60}Co source placed 30º from the D1-D2 axis. Data were selected from within a 1.4 ns ToF window. The ARM was measured for 1.3 MeV photons and found to be 7.3º (FWHM). This value is dominated by the angular size of the D1 and D2 cells at a distance of 15 cm, much closer than they will eventually be. Nevertheless, this ARM value is already better than that of COMPTEL at this energy (Fig. 8). Imposing both ToF and ARM cuts we derived a total energy spectrum (Fig. 13). Both the 1.173 MeV and 1.333 MeV lines are visible; the energy resolution is 5.0% (FWHM) at 1.333 MeV. This resolution is substantially better than that of COMPTEL (Fig. 7). We will continue to work to improve on this value by improving the light collection in both D1 and D2.

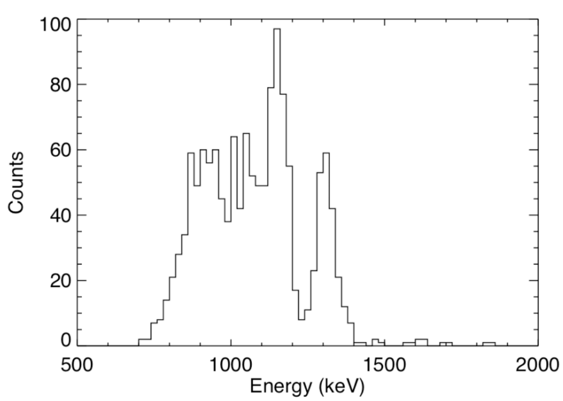

Fig. 13. Total energy spectrum of a ^{60}Co source recorded by the lab prototype. The energy resolution is 5.0% (FWHM) at 1.333 MeV.

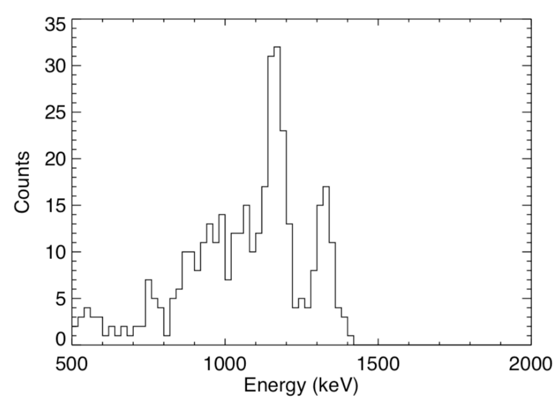

Fig. 14. Simulated total energy spectrum for the lab prototype. The energy resolution is 5.1% (FWHM) at 1.333 MeV, in good agreement with the measurements.

We have performed initial Monte Carlo simulations of the laboratory setup using MGGPOD, using the measured energy resolution of each detector cell to add noise to the simulated hits. Both the ARM distribution and total energy spectrum are reproduced in good agreement with the recorded data (Fig. 14). We will continue to refine our simulations and require good agreement with our laboratory tests. In this way we may reliably predict the performance of the full six-detector prototype and of future, full-scale instruments.

Future laboratory tests will include more complete measurements of the response to gamma rays at different energies and incident angles, and tests of the susceptibility to 2.2 MeV background using laboratory neutron sources.

5.2 Balloon Test Flight

In order to definitively test the background rejection capabilities of the new Compton telescope concept, we will fly the full six-detector prototype on a test balloon flight in the fall of 2010. For this flight we will make use of existing flight hardware that was used for the flight of the GRAPE prototype detector in June 2007[26]. This hardware includes a pressure vessel, six plastic anticoincidence panels with wavelength-shifting bars and readout PMTs, a single-board PC-104 data acquisition computer with custom interface board, a laptop hard drive with backup flash memory, and a simple thermal control system consisting of heaters and fans.

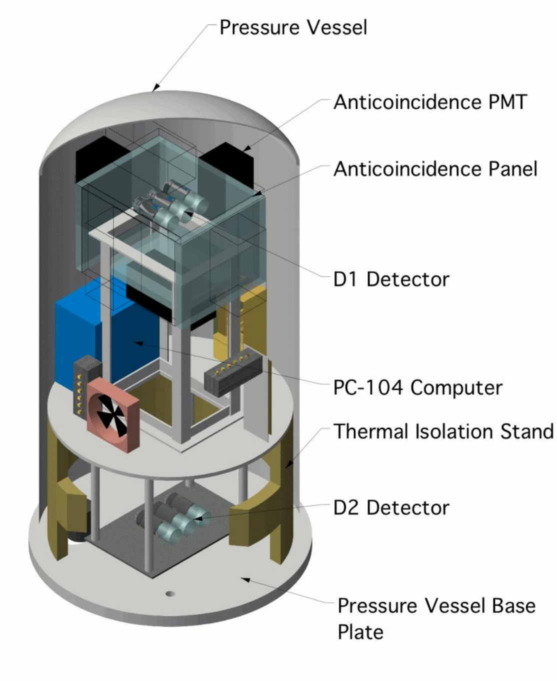

Fig. 15. Drawing of the scintillator Compton telescope balloon payload, scheduled to fly in the fall of 2010.

The Compton telescope payload is shown schematically in Fig. 15. The D1 and D2 layers will contain 2 – 3 detectors each and be placed approximately 50 cm apart. The plastic anticoincidence panels will be placed around the D1 detectors only, since they are not 50 cm long. Custom electronics boards will be designed and fabricated to control the functions of the D1 and D2 detectors. This will be a single PC board with inputs for each PMT for pulse height and pulse shape processing. Anticoincidence veto signals from the shield will be processed as well. Also contained on the board will be the coincidence and ToF logic for valid event determination. The board will include a PIC processor and interface to the PC-104 through a 4-channel RS232. The pulse heights, pulse shape, veto flag, and ToF for each event will be recorded on the laptop hard drive backed up by flash memory.

Before the flight, detailed Monte Carlo simulations of the expected instrumental background will be performed using MGGPOD, including the effects of atmospheric gamma rays and cosmic ray interactions. The recorded background will be compared to the simulations in detail in order to fully understand the instrumental background of the instrument. We will attempt to identify all expected components in the ToF spectrum (Figs. 4 – 5) including, for example, nearly coincident gammas from ^{24}Na produced by activation of the Al pressure vessel (i.e., Type C events). Once the flight background is thoroughly modeled and understood, we will be in a position to predict the performance of a larger instrument carried on an ultra-long duration balloon platform, or of a space-based mission in low earth orbit.

6. CONCLUSIONS

With advancing scintillator technology, significant strides can be made to reduce the effects of background in balloon- and space-borne Compton telescopes. The experience of the COMPTEL experiment provided the data that brought forth the nature of various background components. Each of these components, many individually tailored to the specific background, can be suppressed or greatly reduced with the net effect that the overall instrumental signal-to-noise ratio can improve, in the worst case, by a factor or two and in the best case, by more than a factor of ten. This improvement will result in an instrument capable of surpassing the achievements of COMPTEL in mapping the cosmos for all forms of cosmic gamma-ray sources.

REFERENCES

[1] Ryan, J. M., "Astrophysics challenges of MeV astronomy instrumentation," New Astronomy Reviews, 48, 199 (2004)

[2] Schönfelder, V., et al., "Instrument description and performance of the imaging gamma-ray telescope COMPTEL aboard the Compton Gamma-Ray Observatory," Astrophysical Journal Supplement Series, 86, 657 (1993)

[3] Ryan, J. M., Bloser, P. F., Macri, J. R., McConnell, M. L., "Using LaX Scintillator in a New Low-Background Compton Telescope," Proc. SPIE, 6707, 670703 (2007)

[4] Boggs, S. E., et al., "The Advanced Compton Telescope Mission," http://arxiv.org/abs/astro-ph/0608532 (2006)

[5] Boggs, S. E., "The Advanced Compton Telescope Mission," New Astronomy Reviews, 50, 604 (2006)

[6] McConnell, M.L., et al., "The Soft Gamma-Ray Spectral Variability of Cygnus X-1," Astrophysical Journal, 572, 984 (2002)

[7] Dingus, B.L., "EGRET Observations of > 30 MeV Emission from the Brightest Bursts Detected by BATSE," Astrophysics and Space Science, 231, 187 (1995)

[8] McConnell, M. L., & Ryan, J. M., "Status and prospects for polarimetry in high energy astrophysics," New Astronomy Reviews, 48, 215 (2004)

[9] Diehl, R., et al., "COMPTEL observations of Galactic ^{26}Al emission," Astronomy and Astrophysics, 298, 445 (1995)

[10] Iyudin, A.F., et al., "COMPTEL observations of Ti-44 gamma-ray line emission from CAS A," Astronomy and Astrophysics, 284, L1 (1994)

[11] Morris, D. J., et al., "Reassessment of the ^{56}Co emission from SN 1991T," Proceedings of the Fourth Compton Symposium (AIP 410), 1084 (1998)

[12] Strong, A., et al., "Diffuse continuum gamma rays from the galaxy," Astrophysical Journal, 537, 763 (2000)

[13] Schönfelder, V., et al., "Diffuse cosmic and atmospheric MeV gamma radiation from balloon observations," Astrophysical Journal, 217, 306 (1977)

[14] White, R. S., et al., "Cosmic diffuse gamma rays from 2 to 25 MeV," Astrophysical Journal, 218, 920 (1977)

[15] Ryan, J. M., "Energy and angle distributions for atmospheric and cosmic diffuse gamma rays from 2 to 25 MeV," Ph.D. Thesis, University of California, Riverside (1978)

[16] Bloemen, H., et al., "The revised COMPTEL Orion results," Astrophysical Journal, 521, L137 (1999)

[17] Kappadath, S. C., "Measurement of the cosmic diffuse gamma-ray spectrum from 800 keV to 30 MeV," Ph.D. Thesis, University of New Hampshire (1998)

[18] Weidenspointner, G., "The origin of the cosmic gamma-ray background in the COMPTEL energy range," Ph.D. Thesis, Technical University Munich, Germany (1999)

[19] Weidenspointner, G., et al., "The COMPTEL instrumental line background," Astronomy & Astrophysics, 368, 347 (2001)

[20] Share, G. H., et al., "SMM detection of diffuse galactic 511 keV annihilation radiation," Astrophysical Journal, 326, 717 (1988)

[21] Rozsa, C. M., Menge, P. R., & Mayhugh, M. R., "BriLanCe™ Scintillators Performance Summary," Scintillation Products Technical Note, Saint-Gobain Crystals, http://www.detectors.saint-gobain.com/ (2009)

[22] Shah, K. S., et al., "$LaBr_3$:Ce Scintillators for Gamma Ray Spectroscopy," IEEE Transactions on Nuclear Science, 50, 2410 (2003)

[23] Kuhn, A., et al., "Design of a Lanthanum Bromide Detector for Time-of-Flight PET," IEEE Transactions on Nuclear Science, 51, 2550 (2004)

[24] Owens, A., et al., "Assessment of the radiation tolerance of $LaBr_3$:Ce scintillators to solar proton events," NIM A, 572, 785 (2007)

[25] Weidenspointner, G., et al., "MGGPOD: a Monte Carlo Suite for Modeling Instrumental Line and Continuum Backgrounds in Gamma-Ray Astronomy," Astrophysical Journal Supplement Series, 156, 69 (2005)

[26] Bloser, P. F., et al., "Calibration of the Gamma-RAy Polarimeter Experiment (GRAPE) at a polarized hard X-ray beam," NIM-A, 600, 424-433 (2009)